

G. Hensler
Universitäts-Sternwarte
Geismarlandstr. 11
D-3400 Göttingen

ABSTRACT

A numerical method for 3D magnetohydrodynamical investigations of accretion disks in close binary systems is presented, which allows for good spatial resolution of structures (hot spot, accretion column). The gas is treated as individual gas cells (pseudo-particles) whose motion is calculated within a grid consisting of one spherical inner part for 3D MHD and two plane outer parts. Viscous interactions of the gas cells are taken into account by a special treatment connected with the grid geometry.

We present one result of 2D hydrodynamical calculations for a binary applying the following parameters which are representative for Cataclysmic Variables: $M_1 = 1 M_\odot$, $r_1 = 10^{-2} R_\odot$, $M_2 = 0.5 M_\odot$, $p = 0.2$ d, $\dot{M} = 10^{-9} M_\odot \text{ y}^{-1}$.

Column density and radiative flux distributions over the disk are shown and briefly discussed by comparison with the theoretical understanding of these Dwarf Novae drawn from observations.

I. INTRODUCTION

If in a binary system the one component is filling out its Roche-volume material is transferred through the inner Lagrangian point L_1 towards its companion, which is called the primary or the gainer.

According to Kippenhahn and Weigert (1967) one distinguishes generally between three different cases of mass exchange depending on the evolutionary stage of the mass giving star, henceforth called the secondary or loser (as proposed by Plavec (1980)), extended in the last years to combined cases (e.g. Delgado and Thomas, 1981) due to a better knowledge of stellar evolution in binaries.

The matter streaming through L_1 does not fall radially onto the primary's surface but is deflected due to the Coriolis-force in the corotating frame. Then the increasing gravitational force turns it

again towards the primary, and if the gas stream is able to pass by the primary it turns around and strikes itself.

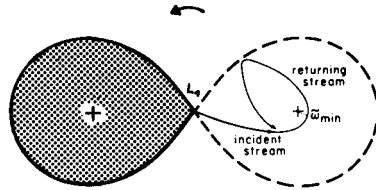


Fig. 1: Stream trajectory for the infalling matter beginning at L_1 . We are looking perpendicular to the equatorial plane with a counter-clockwise direction of rotation. +: centres of gravity of the components, ω_{\min} : minimum distance of the stream from the primary's centre (from Lubow and Shu, 1975)

Because of dissipation mechanisms like viscosity and small scale magnetic fields (Shakura and Sunyaev, 1973; Lynden-Bell and Pringle, 1974) the gas forms a disk where angular momentum is transported outwards so that material flowing inwards can be accreted onto the primary's surface.

Disks in semidetached binaries can be observed e.g. in Cataclysmic Variables (Warner, 1976) and most X-ray binaries (van den Heuvel, 1976; Crampton, 1980) where the primary is already a compact object.

To understand the observations it is necessary to investigate disk structures and the corresponding radiation. Until now only detailed work has been done on these treating special aspects. The crucial problem for disk calculations is not to know the viscosity (Lynden-Bell and Pringle, 1974).

Standard accretion disk models (Shakura and Sunyaev, 1973; Novikov and Thorne, 1973; Lightman, 1974a, 1974b) and investigations concerning the stability of these disks (Shakura and Sunyaev, 1976; Pringle, 1976), the time dependent structure of disks in Cataclysmic Variables (Bath and Pringle, 1981), the vertical disk structure by energy transport considerations (Tayler, 1980; Meyer and Meyer-Hofmeister, 1981), spectral flux distributions (Pacharintanakul and Katz, 1980), and continuum and line spectra (Mayo et al., 1980; and references therein) have made use of the α -prescription introduced by Shakura and Sunyaev (1973) to parametrize the viscosity.

The α -disk model, however, is only valid in the inner region of a disk where the structure is cylindrically symmetric. Asymmetric phenomena produced by hydrodynamical effects in the outer regions like a hot spot, or eccentric orbits of the gas and tidal effects due to the secondary's gravitational influence cannot be considered.

binary system is displayed in Fig. 2. The coordinates are in units of the separation of the two components with the origin at the primary's centre. For simplicity we are calculating in spherical polar coordinates. The following parameters are given:

$Q = \frac{M_1}{M_2}$, the mass ratio of the gainer to the loser, PER (= τ , in the text) the orbital period of the binary system, and A (= d) the resulting separation of the components.

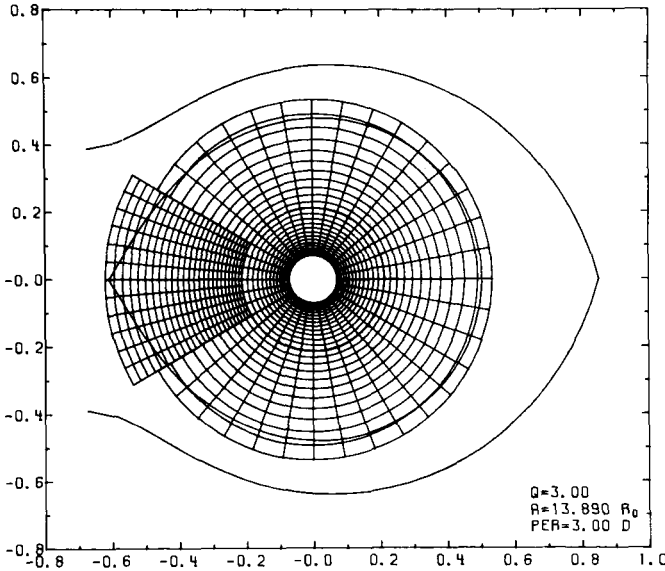


FIG. 2 - THE GRID.

The grid is divided into three parts: a) One spherical part in the inner region which is pinned to the primary because later the magnetic interaction with the matter should be considered within this part, and b) two parts in the outer region, only two-dimensional. The mesh sizes of the grid can be varied separately, but it must be fulfilled that each grid cell is occupied by at least one particle (the PIC method requires an average of 4 - 5 particles per cell) to represent the hydrodynamics. Because the outer grid parts are fixed in the binary system, the inner grid part is able to rotate together with the primary nonsynchronously with respect to the orbital motion.

With the grid we are calculating the pressure gradient. If we consider, for simplicity, three grid cells in the x-direction only and a particle *i* in the middle one (index 2) at x_1 , we express the pressure gradient as

$$\left(\frac{d}{dx}\right)_i^P = \frac{(P_3 - P_2)(x_i - x_2)}{(x_3 - x_2)^2} + \frac{(P_2 - P_1)(x_3 - x_i)}{(x_3 - x_2)^2}, \tag{2}$$

where x_2 and x_3 denote the location of the cell boundaries between the cells. Test calculations for a hydrostatic stratification have confirmed this form.

The most important reason for introducing a grid was to consider a viscous interaction of the particles. It consists of two steps:

1) for each grid cell the particle velocities \underline{u}_i are altered by

$$\underline{u}_i^{\text{new}} = \underline{u}_i^{\text{old}} (1 - f_v) + \bar{\underline{u}}_g \cdot f_v, \tag{3}$$

where $\bar{\underline{u}}_g$ denotes the averaged velocity of the grid cell in question conserving the angular momentum there. f_v is the viscosity parameter in the range from 0. to 1. If we apply this first viscous interaction in our circular grid with vanishing pressure forces, a circular disk would be unable to transport angular momentum radially due to Keplerian particle orbits.

2) Therefore, the velocities are smeared over all adjoining grid cells according to the PIC method (Potter, 1973). The new particle velocity is then computed by

$$\underline{u}_i^{\text{new}'} = \underline{u}_i^{\text{new}} (1 - f_v) + \bar{\underline{u}}_{\text{ad}} \cdot f_v, \quad 0 \leq f_v \leq 1 \tag{4}$$

The mean velocity (see Fig. 3)

$$\bar{\underline{u}}_{\text{ad}} = \frac{\sum_{i,j} a_{i,j} \cdot \rho_{i,j} \cdot \bar{\underline{u}}_{i,j}}{\sum_{i,j} a_{i,j} \cdot \rho_{i,j}}, \quad A_g = \sum_{i,j} a_{i,j} \tag{5}$$

also prevents large differences in the fluid velocity of neighbouring grid cells.

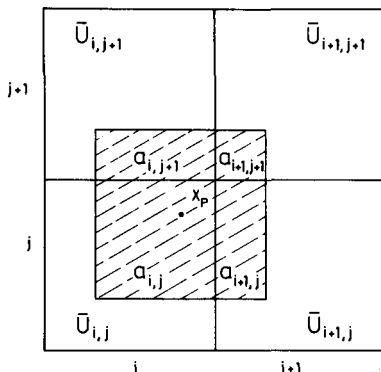


Fig. 3:
2D-interpolation for a 'particle' velocity with the four nearest grid cells. x_p : 'particle' location, $a_{i,j}$: fractions of areas around the 'particle' overlapping with the grid cells, $\bar{\underline{u}}_{i,j}$: mean velocity of the grid cells (cf. Potter, 1973, p. 159)

To calculate the gas stream, particle calculations in the restricted three-body problem without any interaction of the particles were conducted by several investigators (for references see the following authors) but cannot represent the hydrodynamics realistically. Also the following hydrodynamical calculations (Prendergast, 1960; Biermann, 1971; Prendergast and Taam, 1974; Lubow and Shu, 1975; Sørensen et al., 1975; Flannery, 1975; Lin and Pringle, 1976) have been carried out either without taking any viscous interaction into account or treating the energy equation only very crudely. The most successful work was done by Lin and Pringle (1976) where the gas is treated as individual gas cells moving in a cartesian grid. This, however, yields an anisotropic viscosity. They did not investigate various disk structures for different viscosities because they only intended to show a method for numerical calculations of disk structures and its feasibility. Standard hydrodynamical finite difference methods as recently also applied by Everson (1981) to time dependent accretion disks are not very suitable because of the limited spatial resolution of the grid due to the rigid grid shape, inability to adjust to the different hydrodynamical structures, and due to the limitation of computer storage.

II. BASIC EQUATIONS AND NUMERICAL METHOD

Because in many cases the primary has a magnetic field, we are also interested in the interaction of the magnetic field with the matter in the disk. In order to include this effect later, my intention was to develop a numerical method which should allow three-dimensional MHD computations, improve the coupled treatment of hydrodynamics and energy equation, and be applicable to a large range of parameters.

Most promising seemed to me the use of a pseudo-particle method (see e.g. for the "smoothed particle hydrodynamics" (SPH) Lucy (1977), for the "particle-in-cell" method (PIC) Harlow (1964), and for 3D MHD Leboeuf et al. (1979)).

We divide the gas into individual gas cells which carry not only mass but also internal energy with them. Until now we have calculated only two-dimensionally, ignoring for the moment magnetic fields. As we are dealing with pseudo-particles, the momentum equation in the corotating system is expressed in Lagrangian form,

$$\frac{Du}{Dt} = -\nabla\phi - \underline{\omega} \times (\underline{\omega} \times \underline{r}) - 2\underline{\omega} \times \underline{u} - \frac{1}{\rho} \nabla P + \nu \Delta \underline{u} \quad , \quad (1)$$

Here, \underline{r} and \underline{u} are the particle's location and velocity, respectively. ϕ consists of the potentials of both components. ω is the angular velocity $2\pi/\tau$ (τ : the orbital period) with its vector directed perpendicularly to the rotational plane. ρ denotes the density, P the pressure, and ν the kinematic viscosity.

To calculate e.g. the viscous interaction, besides the particles we introduce a rough grid which fills out the Roche-lobe of the primary. The crosscut of the grid with the rotational plane of the

Test calculations for a viscous isothermal compressible gas flow between two fixed parallel walls have shown the expected stream profiles. Concerning our input parameters which determine the viscosity, the test calculations also show that the kinematic viscosity ν is proportional to the area of the grid cell A_g and nearly proportional to the square root of our viscosity parameter f_ν .

$$\nu \sim A_g \cdot f_\nu^{1/2} \quad (6)$$

To calculate disk models with an almost constant kinematic viscosity we accomplish this by taking advantage of this proportionality.

Because the molecular velocity is too inefficient to transport enough angular momentum to yield a broad disk it is generally accepted (Shakura and Sunyaev, 1973, 1976; Lynden-Bell and Pringle, 1974) that the gas flow must be unstable against turbulence.

The energy transport combined with turbulent motion is treated in the same way as the viscous interaction. The internal energy e_i of a particle is computed in two steps:

1) Inside each grid cell by

$$e_i^{\text{new}} = \frac{\epsilon_g^{\text{new}}}{\rho_g} f_\chi + \frac{E_g^{\text{new}}}{E_g^{\text{old}}} e_i^{\text{old}} (1 - f_\chi) \quad , \quad (7)$$

where ϵ_g is the internal energy density and E_g the internal energy of the grid cell in question. The upper index ("old" and "new") denotes the internal energy before and after energy dissipation by viscosity, respectively. ρ_g is the particle density of the grid cell g and f_χ the efficiency factor of the energy transport ($0. \leq f_\chi \leq 1$).

2) Over the adjoining grid cells by

$$e_i = (1 - f_\chi) e_i^{\text{new}} + f_\chi \bar{e}_{\text{ad}} \quad (8)$$

with

$$\bar{e}_{\text{ad}} = \frac{\sum_{i,j} a_{i,j} \cdot \epsilon_{i,j}}{\sum_{i,j} a_{i,j} \cdot \rho_{i,j}} \quad (9)$$

Assuming the Prandtl number $Pr = \frac{\nu}{\chi}$ to be of order unity for a perfect gas we perform the calculations with $f_\chi = f_\nu$.

The energy change due to the work done by pressure, $-P\bar{V}u$, is taken into account similar to the following expression (in dimensionless form), where we again consider only the one-dimensional cartesian case, for simplicity:

$$\frac{dE_2}{dt} = -E_2 \left(\frac{u_3 - u_1}{\Delta x} \right) \tag{10}$$

We obtain the vertical density stratification ρ using the momentum equation (1) in vertical direction z (neglecting the viscosity term) (see Hensler, 1981a) and the pressure P by the perfect gas law. Because we are not interested in the vertical disk structure (for α -disks see Meyer and Meyer-Hofmeister, 1981) but only in mean values of ρ , P , and T , we assume the temperature T to be constant in the vertical direction and determine it by the assumption of energy balance. Shakura and Sunyaev (1976) and Pringle (1976) confirmed this to be realized in α -disks.

With the further assumption of an optically thick disk the radiation flux from one disk surface

$$Q_{\text{rad}} = \frac{Q_z}{A_g \cdot \Delta t} = \frac{8 \sigma T^4}{3 \kappa \Sigma} \tag{12}$$

and Kramer's opacity formula

$$\kappa = 0.4 + 3.2 \times 10^{22} \frac{\rho}{T^{3.5}} \tag{13}$$

determine the equilibrium temperature T . Here σ is the Stefan-Boltzmann constant and Σ the surface or column density.

III. COMPUTATIONS

According to the mass transfer rate \dot{M} through the inner Lagrangian point L_1 , gas cells are initiated randomly in constant time steps in the vicinity of L_1 having an initial velocity of 10 km s^{-1} in the negative radial direction, which is about the sound speed in giant envelopes. The particles are considered in the computation as long as their position is in between the primary's radius r_a and twice the distance of the inner Lagrangian point r_{L_1} . They are omitted if they reach the secondary's Roche-lobe.

If the number of the particles in the system remains constant, we have achieved the stationary state of the disk.

The primary is assumed to rotate synchronously. The influence of nonsynchronous rotation will be discussed elsewhere (Hensler, 1981b). The radiation field of the primary is taken into account within the innermost grid part, that of the secondary for the initiated particles around L_1 .

IV. A DISK MODEL FOR CATAclySMIC VARIABLES

To apply the numerical method described above to binary systems in mass exchange, among other models (Hensler, 1981b) we have calculated a disk model for the Cataclysmic Variables (CVs) represented by a system of the following parameters:

primary's mass	$M_1 = 1 M_{\odot}$
primary's radius	$r_1 = 10^{-2} R_{\odot}$
primary's effective temperature	$T_{\text{eff},1} = 5000 \text{ K}$
secondary's mass	$M_2 = 0.5 M_{\odot}$
orbital period	$\tau = 0.2 \text{ d}$
mass transfer rate	$\dot{M} = 10^{-9} M_{\odot} \text{ y}^{-1}$

From that the mass ratio amounts to $q = 2$, and the separation of the components to $d = 1.65 R_{\odot}$. The period denotes a system which is located at larger values of the period gap of the CVs (Warner, 1976).

Though our method would be applicable also to the time evolution of disks (Hensler, 1981b) (as published by Bath and Pringle (1981) for CVs) we only want to calculate the steady state accretion disk. Therefore, here we are not interested to investigate the outburst mechanism for CVs in order to prefer one of the theories discussed (whether there are mass transfer variations (Bath, 1975; Wood, 1977) or disk instabilities (Osaki, 1974)).

In Fig. 4 the column density distribution is displayed. The parameters are those given before ($Q = q$, $A = d$, $\text{PER} = \tau$, $\text{DM} = M$), and T is the time in units of the period τ .

The density distribution reveals a (horn-like) ring of maximum density with a shallow decrease inwards but an immediate contact of the disk with the primary's surface. The mass accretion rate remains constant and amounts to more than 95 per cent of the transferred material. Only a small inner disk region is circular and almost Keplerian, while the main disk shows an elliptical form due to hydrodynamical structures. The density is decreasing outwards and the disk is filling the whole Roche area, through this cannot be recognized easily from the picture.

From the outer disk region mass loss, combined with angular momentum loss, takes place. Besides this, angular momentum from the disk is also transferred into orbital motion via tidal friction, in this case as efficiently as estimated by Lin and Pringle (1976) and Pappalozou and Pringle (1978) (results for other systems see also Hensler (1981b)).

The radiation flux distribution (Fig. 5) shows nearly the same structure as the density, but a monotonic increase towards the primary's surface. This is due to an increase in released potential energy and prevails over the density decrease there. No hot spot is obtained where it would be expected.

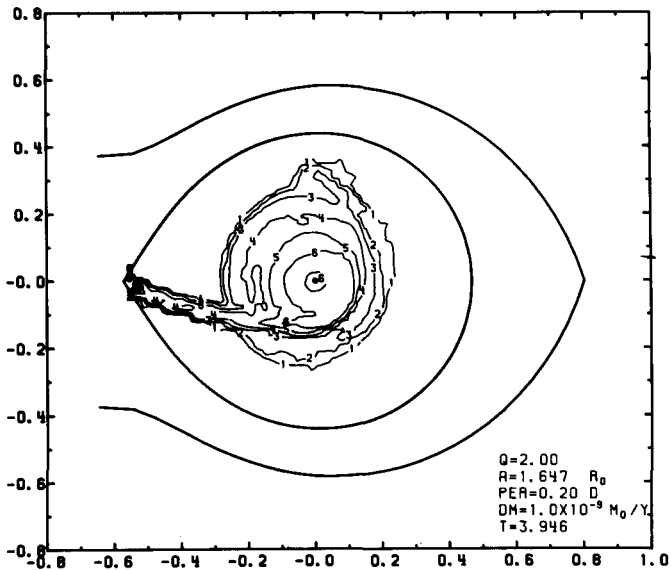


FIG. 4 - COLUMN DENSITY CONTOURS. CONTOUR LABELS CORRESPOND TO
 1: 3.20×10^{22} 2: 5.60×10^{22} 3: 1.00×10^{23}
 4: 1.80×10^{23} 5: 3.20×10^{23} 6: 5.60×10^{23}
 7: 1.00×10^{24} 8: 1.80×10^{24} 9: 3.20×10^{24}
 PARTICLES / CM².

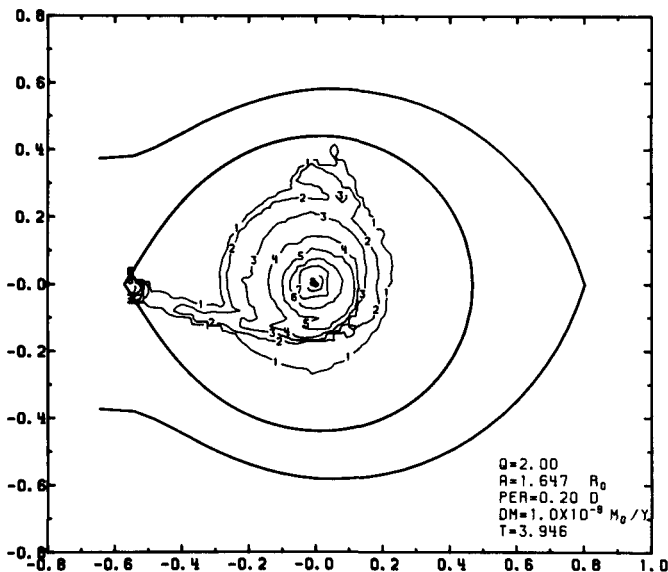


FIG. 5 - RADIATION FLUX. CONTOUR LABELS CORRESPOND TO
 1: 1.00×10^{11} 2: 3.20×10^{11} 3: 1.00×10^{12}
 4: 3.20×10^{12} 5: 1.00×10^{13} 6: 3.20×10^{13}
 7: 1.00×10^{14} 8: 3.20×10^{14} 9: 1.00×10^{15}
 ERG / SEC / CM².

According to the outburst mechanism discussed by Osaki (1974) due to disk instability this disk model would represent accretion in outburst. As known from observations (Warner, 1976) the disk in outburst is brighter and larger than in quiescence, and no hot spot is detectable in the light curve during eclipse (e.g. for OY Car see Vogt, 1979) due to the bright inner disk region. However, if the viscosity is as large as expected for the outburst phase (Osaki, 1974) the infalling matter does not strike denser parts of the disk before its velocity vector nearly coincides with the azimuthal velocity vector of the disk, and kinetic energy is dissipated only over a large region and in tongue-like structures towards the infalling gas stream due to deceleration already in less dense regions. In this case no hot spot exists.

Because the total mass in the disk (Fig. 4) amounts to $10^{-12} M_{\odot}$, in fact the viscosity seems to be somewhat too large with regard to observed accretion disks in CVs where Lin and Pringle (1977) have derived a mean total mass of about $10^{-10} M_{\odot}$.

Opposite the infalling gas stream a warm region is revealed, which seems from observations to be much more prominent in some CVs during quiescence (Haefner and Metz, 1981).

V. CONCLUSIONS

As one sees from the results, the numerical method presented here enables us to calculate hydrodynamical effects in accretion disks which cannot be treated by the α -disk model because of asymmetries and cannot be resolved spatially by finite difference methods. This advantage will be enhanced if we proceed to three-dimensional magnetohydrodynamics which would require only a moderate increase of the particle number in this pseudo-particle method but is not feasible by other hydrodynamical methods with the same spatial resolution. The main problems of the treatment of the viscosity are naturally not solved by this method but are certainly simplified by depending on the mesh size and viscosity parameter. Because the viscous interaction is applied in every time step which is determined by the Courant-Friedrichs-Lewy condition and, therefore, not constant, so far in the calculations the kinematic viscosity ν is also time dependent. However, this is negligible in the case of steady state accretion.

The density decrease from a ring of maximum density inwards is in contradiction to the α -disk (Bath and Pringle, 1981) but I suggest that this is due to the boundary condition of the primary's surface. The deceleration of the particles in the vicinity of the surface and, therefore, the angular momentum transfer from the innermost disk to the star might tend to deplete the boundary layer between disk and surface (Kippenhahn and Thomas, 1978). Furthermore, the enhanced release of potential energy combined with a decrease in disk height inwards diminishes the density, assuming radial pressure balance there.

During the calculation the spin-up of the angular momentum and mass gaining primary is not taken into account, because the time intervals are too short.

The model of an accretion disk presented here for the CVs should only be understood to be one possible disk. Current calculations are carried out to investigate the dependence of the disk structure on the system parameters and especially on the viscosity.

More detailed discussions about the numerical method and some other results can be found in two forthcoming papers (Hensler 1981a, b).

Acknowledgements:

The author is indebted to W. Glatzel, Drs. F. Meyer, H. Ritter, and M. Schüssler for many helpful discussions. The calculations have been carried out on the UNIVAC 1100/82 of the Gesellschaft für wissenschaftliche Datenverarbeitung, Göttingen.

References:

- Bath, G.T.: 1975, *Monthly Notices Roy. Astron. Soc.* 171, 311
 Bath, G.T., Pringle, J.E.: 1981, *Monthly Notices Roy. Astron. Soc.* 194, 967
 Biermann, P.: 1971, *Astron. Astrophys.* 10, 205
 Crampton, D.: 1980, *IAU Symp. No. 88*, p. 313
 Delgado, A.J., Thomas, H.-C.: 1981, *Astron. Astrophys.* 96, 142
 Everson, B.L.: 1981, preprint
 Flannery, B.P.: 1975, *Astrophys. J.* 201, 661
 Haefner, R., Metz, K.: 1981, *Astron. Astrophys.*, in press
 Harlow, F.H.: 1964, *Methods in Comput. Physics Vol. 3*, p. 319
 Hensler, G.: 1981, *Proceed. V. Göttingen-Jerusalem-Symp.*, in press
 Hensler, G.: 1981, this colloquium, p. 219.
 Hensler, G.: 1981a, *Astron. Astrophys.*, submitted
 Hensler, G.: 1981b, *Astron. Astrophys.*, submitted
 Heuvel, E.J.P. van den: 1976, *IAU Symp. No. 73*, p. 35
 Kippenhahn, R., Weigert, A.: 1967, *Z. Astrophys.* 65, 251
 Kippenhahn, R., Thomas, H.-C.: 1978, *Astron. Astrophys.* 63, 265
 Leboeuf, J.N., Tajima, T., Dawson, J.M.: 1979, *J. Comput. Physics* 31, 379
 Lightman, A.P.: 1974a, *Astrophys. J.* 194, 419
 Lightman, A.P.: 1974b, *Astrophys. J.* 194, 429
 Lin, D.N.C., Pringle, J.E.: 1976, *IAU Symp. No. 73*, p. 237
 Lin, D.N.C., Pringle, J.E.: 1977, in "Novae and Related Stars", *Astrophys. Space Sci. Libr. Vol. 65*, ed. M. Friedjung, Reidel, Dordrecht, p. 35
 Lubow, S.H., Shu, F.H.: 1975, *Astrophys. J.* 198, 383
 Lucy, L.B.: 1977, *Astron. J.* 82, 1013
 Lynden-Bell, D., Pringle, J.E.: 1974, *Monthly Notices Roy. Astron. Soc.* 168, 603
 Mayo, S.K., Wickramasinghe, D.T., Whelan, J.A.J.: 1980, *Monthly Notices Roy. Astron. Soc.* 193, 793
 Meyer, F., Meyer-Hofmeister, E.: 1981, *Astron. Astrophys.*, in press

- Novikov, I., Thorne, K.S.: 1973, in "Black Holes", Les Houches 1972, eds. C. DeWitt & B.S. DeWitt, Gordon & Breach, New York, p. 343
- Osaki, Y.: 1974, Publ. Astron. Soc. Japan 26, 429
- Pacharintanakul, P., Katz, J.I.: 1980, *Astrophys. J.* 238, 985
- Papaloizou, J., Pringle, J.E.: 1977, *Monthly Notices Roy. Astron. Soc.* 181, 441
- Plavec, M.J.: 1980, IAU Symp. No. 88, p. 1
- Potter, D.: 1973, "Computational Physics", John Wiley & Sons, London
- Prendergast, K.H.: 1960, *Astrophys. J.* 132, 162
- Prendergast, K.H., Taam, R.E.: 1974, *Astrophys. J.* 189, 125
- Pringle, J.E.: 1976, *Monthly Notices Roy. Astron. Soc.* 177, 65
- Shakura, N.I., Sunyaev, R.A.: 1973, *Astron. Astrophys.* 24, 337
- Shakura, N.I., Sunyaev, R.A.: 1976, *Monthly Notices Roy. Astron. Soc.* 175, 613
- Sørensen, S.-A., Matsuda, T., Sakurai, T.: 1975, *Astrophys. Space Sci.* 33, 465
- Taylor, R.J.: 1980, *Monthly Notices Roy. Astron. Soc.* 191, 135
- Vogt, N.: 1979, *ESO Messenger* 17, 39
- Warner, B.: 1976, IAU Symp. No. 73, p. 85
- Wood, P.R.: 1977, *Astrophys. J.* 217, 530